European Journal of Medicinal Chemistry 102 (2015) 403–412

Contents lists available at ScienceDirect

European Journal of Medicinal Chemistry

journal homepage: http://www.elsevier.com/locate/ejmech

Research paper

Synthesis of new indole-based bisphosphonates and evaluation of their chelating ability in PE/CA-PJ15 cells

Carlo A. Palmerini [a], Francesco Tartacca [a], Michela Mazzoni [a], Letizia Granieri [a], Laura Goracci [b], Angela Scrascia [b], Susan Lepri [b, *]

[a] Department of Agricultural, Food and Environment Science (Unit Research of Biochemistry and Molecular Biology), University of Perugia, via Del Giochetto, 06125 Perugia, Italy
[b] Department of Chemistry, Biology and Biotechnology, University of Perugia, via Elce di Sotto, 8, 06123 Perugia, Italy

ARTICLE INFO

Article history:
Received 1 April 2015
Received in revised form
22 July 2015
Accepted 8 August 2015
Available online 12 August 2015

Keywords:
Indole based bisphosphonate
Cytosolic calcium
Ene reaction
Chelating ability assessment

ABSTRACT

Bisphosphonates are the most important class of antiresorptive agents used against osteoclast-mediated bone loss, and, more recently, in oncology. These compounds have high affinity for calcium ions (Ca^{2+}) and therefore target bone mineral, where they appear to be internalized selectively by bone-resorbing osteoclasts and inhibit osteoclast function. They are extensively used in healthcare, however they are affected by severe side effects; pharmacological properties of bisphosphonates depend on their molecular structure, which is frequently the cause of poor intestinal adsorption and low distribution. In this work we synthesized six novel bisphosphonate compounds having a variably substituted indole moiety to evaluate their extra- and intracellular calcium chelating ability in PE/CA-PJ15 cells. Preliminary *in silico* and *in vitro* ADME studies were also performed and the results suggested that the indole moiety plays an important role in cell permeability and metabolism properties.

© 2015 Elsevier Masson SAS. All rights reserved.

1. Introduction

Bisphosphonates (BPs) are analogs of naturally occurring pyrophosphates and represent an important class of drugs, used to treat conditions such as osteoporosis, Paget's syndrome and some tumors [1,2]. Similarly to inorganic pyrophosphate, BPs antagonize the dissolution of hydroxyapatite crystals and the metastatic calcification of tissues, however unlike their endogenous analogs they are not cleaved by pyrophosphatase [3,4]. The biological activity of BPs largely depends on the Ca^{2+}-chelating properties of the two phosphate groups. As it is widely known, calcium is used in cellular signaling: in eukaryotic cells the ion is sequestered in cellular organelles (such as endoplasmic reticulum and mitochondria) and it is released according to the cell activation [5]. Cytoplasmic Ca^{2+} concentration $[Ca^{2+}]_c$ is very low ($\approx$100 nM) compared to that in the extracellular medium ($\approx$1 mM). The maintenance of such a calcium concentration gradient between the cytosol and other compartments is crucial for cells survival [6]. Calcium homeostasis is finely tuned through various mechanisms [7]; an uncontrolled Ca^{2+} signal may alter secretion, contraction, protein activity, apoptosis, proliferation and other critical processes [8].

BPs can be distinguished in two classes: the non-nitrogen-containing bisphosphonates (NNBPs) and the nitrogen-containing bisphosphonates (NBPs) [9]. Etidronate (ETD) and clodronate (CLD) (Fig. 1) belong to the NNBPs family, and they are known to block ATP-dependent enzymes able to induce the death of the osteoclast [10]. Alendronate (ALN), risedronate (RSD), and pamidronate (PMD) (Fig. 1) belong to the NBPs class, and are inhibitors of the farnesyl pyrophosphate synthase [2]. These drugs inhibit the prenylation of GTPase-dependent proteins (Ras, Rab, Rho and Rac) that are essential for the osteoclast's survival. The deterioration of cytoskeleton of these cells does not allow the formation of the ruffled border, causing their apoptosis [11,12].

Survival time, proliferation, adhesion and migration are the main effects of NBPs on tumor cell lines "*in vitro*" [13,14] and most of these effects are due to the inhibition of farnesyl pyrophosphate synthetase [15]. In addition, the inhibition of protein prenylation may alter the viability and the proliferation of endothelial cells *in vitro* [16]. Studies on mice indicate that NBPs inhibit the formation of bone metastases and decrease bone mass *in vivo* [16,17], suggesting a relationship between their antitumor effects and their cellular uptake *in vivo*. NBPs induce a pre-apoptotic action on

* Corresponding author.
E-mail address: susan@chemiome.chm.unipg.it (S. Lepri).

http://dx.doi.org/10.1016/j.ejmech.2015.08.019
0223-5234/© 2015 Elsevier Masson SAS. All rights reserved.

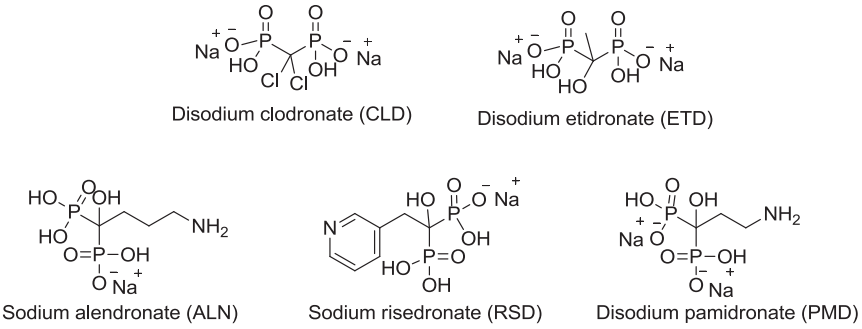

Fig. 1. Chemical structure of commercially available bisphosphonate drugs in their sodium salt form (clodronate, etidronate, alendronate, risedronate, and pamidronate).

neoplastic cancer cells and inhibit the mechanisms regulating the cellular proliferation and adhesion [14,15].

The major drawback of NBP drugs is their high hydrophilicity and polarity. Thus, many common NBP drugs demonstrate poor cell-membrane permeability towards tumor cells and other non-endocytic cells [18,19]. The uptake and binding to bone mineral is determined by the presence of the bisphosphonates moiety, while the substituents bound to the P–C–P moiety are thought to be essential to ensure satisfactory antiresorptive potency. Thus, small changes in the substituents of the P–C–P moiety may influence the resorption properties [20].

Another consequence of the high hydrophilicity of NBPs is their metabolic stability. Indeed, they are not metabolized by CYP450 or other phase I enzymes [21], and are mostly eliminated unchanged in urine [20]. On one hand, an extensive metabolism of a drug might jeopardize its pharmacological activity; on the other hand, when drugs are substrates for CYP450 enzymes, their half-life, as well as the pharmacological and toxicity effects, can be modulated by synthetic modifications.

As mentioned above, residual bisphosphonates which are not taken up by the bones are excreted in urine without being unmetabolized. As a consequence, a common adverse event related to bisphosphonate drugs is nephrotoxicity. In fact, pharmacokinetic and pharmacodynamic properties (see Table 1 for pK_a, LogP, and oral bioavailability data), modulate the bisphosphonates accumulation which is related to renal histopathology. Even though a low dose is usually well tolerated, the high dose required in an oncology setting is often correlated to nephrotoxicity [22]. In particular, the major toxicity effects seem correlated to intravenous administration of BPs. In addition, orally administered BPs are often correlated with adverse effects on gastrointestinal tract, such as ulceration in esophagus, stomach and duodenum. Other adverse events such as acute-phase reactions, and the osteonecrosis of the jaw have also been observed [23]. Thus, the improvement of the pharmacokinetic properties of bisphosphonates retaining the desired biological effect represents a valuable strategy to obtain novel series of safer bisphosphonate drugs.

Thus, in this work six novel indole-based bisphosphonates (IBPs) (compounds **1a**–**f**, Fig. 2) were synthesized and investigated for their ability in chelating extracellular and cytosolic calcium in the PE/CA P-J15 cells as a function of both the nature and the position of the substituent in the indole nucleus. In particular, owing to the interesting role played by fluorine in bioactive molecules [29–31], four fluorinated compounds were investigated. The PE/CA-PJ15 cells are obtained from human oral squamous cancer cells; they are similar to epithelial cells and express laminin and cytokeratins [32] and are responsible for about 90% of head and neck tumors. Our results showed that two out of six indole-bisphosphonates were significantly more effective than the commercially available ALN and CLD in chelating Ca^{2+}. The *in silico* evaluation of the passive cell membrane permeation ability suggested that the Ca^{2+}-binding efficacy of these compounds may be related to an increased cell permeability. Finally, the metabolic stability in human liver microsomes was determined for the most promising compounds, which, conversely to the ALN and CLD compounds, were rapidly metabolized.

Table 1
Experimental pK_a, LogP and oral bioavailability data of commercial BPs.

Comp.	pK_{a1-5}[a]	LogP[b] [24]	Oral bioavailability %[b] [25]
CLD	1.7, 2.1, 5.7, 8.3 [25]	−2.4	1–2
ETD	1.7, 2.5, 7.2, 10.8 [26]	−3.8	3–7
ALN	1.3, 2.2, 6.4, 11.0, 11.8 [27]	−4.3	0.75
RSD	1.6, 2.2, 5.9, 7.1, 11.7 [28]	−3.6	0.65
PMD	1.2, 1.9, 6.0, 10.2, 12.1 [27]	−4.7	0.3

[a] Related to respective acid form.
[b] Referred to commercial salt form.

2. Results and discussion

2.1. Synthesis of indole-based bisphosphonates

The indole nucleus is a well-established pharmacophore present in many synthetic and natural drugs with remarkable biological activities [10] and indole containing bisphosphonates have already been assessed for their anti-bone resorptive activity in bone marrow osteoclast culture [33].

As previously reported, 3-methyleneindolines are valuable building blocks for 3-functionalized indole derivatives due to the remarkable reactivity of the exocyclic carbon–carbon double bond through the “ene” reaction [34,35]. These findings led us to consider their use for the synthesis of new regioselectively substituted tetraethyl [3-(1*H*-indol-3-yl)propane-1,1-diyl] bis(phosphonate) derivatives **1a**–**f** with Ca^{2+} chelating ability and improved cell permeability (Fig. 2). The *N*-Boc protected 3-methyleneindolines **5a**–**f** were prepared in four steps, starting from commercially available substituted anilines (Scheme 1). When not commercially available, *o*-bromoanilides **3** were obtained by metalation of the *N*-Boc-protected anilines **2**, followed by treatment of the resulting dilithiated anilide intermediate with CBr_4. NaH-promoted deprotonation of anilide **3** in DMF, followed by the reaction with propargyl bromide, gave the corresponding *N*-propargyl derivatives **4** in good yield. Finally, the reductive radical cyclization of *N*-bromoaryl-*N*-propargylcarbamate with tributhyltin hydride in refluxing benzene, in the presence of AIBN initiator, provided the expected 3-methyleneindoline **5** in satisfactory yields. 3-Methyleneindolines **5** are relatively stable at room temperature and can be purified by standard chromatographic

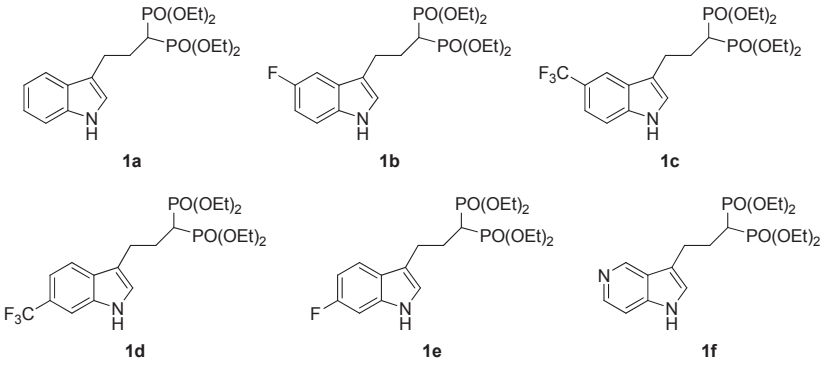

Fig. 2. Chemical structure of novel indole-based bisphosphonates (IBPs, **1a**–**f**).

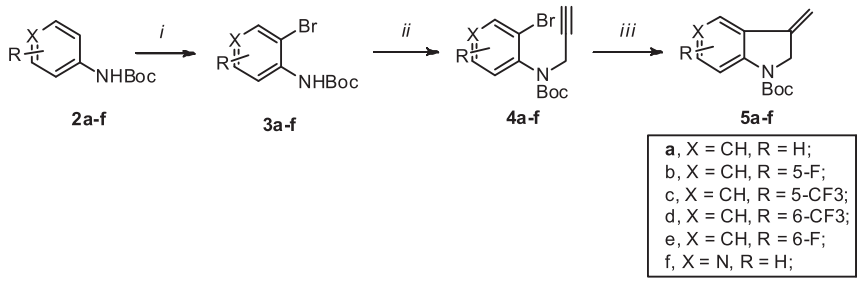

[a]Reagents and conditions: (*i*) 1. *n*-BuLi, THF, -78°C; 2. CBr_4 (52–94%); (*ii*) NaH, propargyl bromide, DMF (61–86%); (*iii*) AIBN, Bu_3SnH, benzene reflux, 3h (10–69%).

Scheme 1. Synthesis of regiosubstituted 3-methyleneindolines.

methods without any isomerization to the corresponding 3-methylindoles.

Owing to the presence of two powerful electron-withdrawing phosphoryl groups, alkyl vinylidene gem-bisphosphonates (VBP) [36] are very electrophilic species. They have been employed in the synthesis of several alkyl bisphosphonates as Michael-type nucleophile acceptors [37] as well as in Lewis acid-catalyzed Friedel–-Crafts reactions with activated aromatics [38–40] and seldom as dienophile in Diels–Alder cycloaddition. However, to our knowledge, VBP has never been used as an enophile in *ene*-type reactions. Indeed, according to NMR spectra (see Supporting Information), indolylalkylbisphosphonate (IBPs) **1a**–**f** can be easily obtained in 50–70% yield by simple heating an equimolar mixture of the suitable Boc-protected 3-methyleneindoline and VBP [41] at 100 °C for 2–4 h in solvent-free conditions (Scheme 2). The protecting *tert*-butoxycarbonyl group is easily removed by simply rising the temperature to 150–190 °C until complete nitrogen deprotection to give final compounds **1a**–**f** (Scheme 2). The structures of the bisphosphonates **5a**–**f** and **1a**–**f** were confirmed by spectroscopic methods. In particular, the presence of the P–CH–P moiety was supported by the presence of a typical triplet peak ($\delta \approx 35$ ppm, $J \approx 130$ Hz) in the ^{13}C NMR spectra. The molecular formulas were obtained by ESI HRMS, and all compounds were fully characterized by ^{1}H, ^{13}C, ^{19}F and ^{31}P NMR spectroscopy (See Supplementary Information). As an example, 2D NMR spectra and NMR assignments for compound **1a** are reported in Supplementary Information.

Table 2
Predicted pK_a and LogP for compounds **1a**–**f**.

Comp.	pK_a[a]	LogP[b]
1a	>15	2.9
1b	>15	3.1
1c	>15	3.8
1d	>15	3.8
1e	>15	3.1
1f	7.96	1.8

[a] Predicted using MoKa 2.6 [46].
[b] Predicted using VolSurf+ [47].

The predicted pK_a and LogP for the synthesized compounds **1a**–**f** are reported in Table 2. It is immediately evident that the synthesized compounds possess very different physicochemical

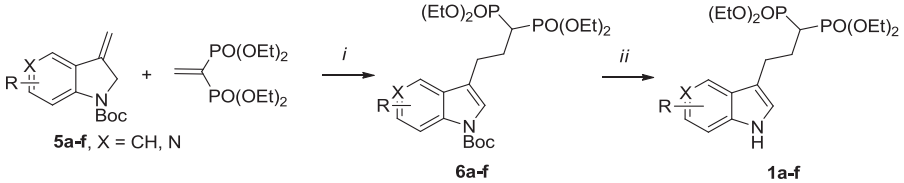

[a]Reagents and conditions: (*i*) 100°C, 2–4 h (52-75%); (*ii*) 150-190°C, 5–10 min (99%).

Scheme 2. [a]Synthesis of regiosubstituted substituted IBPs by "ene" reactions.

properties with respect to commercial BPs. Indeed, they lack the acid features, although compounds **1a**–**f** could act as prodrugs with subsequent ester cleavage. Other attempts to synthesized BPs prodrugs have been proposed [25] suggesting that several groups (such as carboxylic esters, amides, anhydrides) can be used to functionalize the acid phosphate in order to improve the compound's oral bioavailability. The presence of the indole scaffold and the esterification of the bisphosphonate moiety also results in a significant increase of the LogP value. For compound **1f**, a basic pK_a of 7.96 is also predicted for the azaindole scaffold.

According to literature protocols [40], few attempts to obtain the free bisphosphonic acid derivatives have been made to experimentally evaluate the effect of the ester group (e.g. Scheme SI1). However, under this condition, the expected acid was obtained as minority product (14%), while the 2,2-coupled dihydrodimer was observed (see Supporting Information for further details). Such couplings are known for simple indole, skatole, and other 3-substituted indoles under acidic condition [42–45].

2.2. Biological evaluation of indole-based bisphosphonates

The Ca^{2+} chelating ability of indole-based bisphosphonates 1a–f was tested using PE/CA-PJ15 cells. This cell line is obtained from squamous cell tongue carcinoma, which accounts for about 90% of head and neck tumors. These cells, similar to epithelial cells, express laminin and cytokeratins [32,48]. In this study, we investigated the impact of synthesized compounds 1a–f on $[Ca^{2+}]_c$ homeostasis in the oral cancer PE/CA-PJ15 cell model to better characterize a biochemical/biological link that may have implications in cell signaling events associated with cell viability and apoptosis in human oral squamous carcinoma.

2.2.1. Bisphosphonates (BPs) chelating ability of extracellular calcium ion

The chelating ability of each novel IBP toward extracellular calcium ions was evaluated using the fluorescent indicator Fura-2, and commercial ALN and CLD were used as reference compounds. Bisphosphonates **1a**–**f** and commercial ALN and CLD were added to a suspension of PE/CA-PJ15 cells in HBSS (Hanks' Balanced Salt Solution, 1 mM $CaCl_2$) buffer previously lysed with 1% Triton X-100. The variation of the Ca^{2+}/FURA complex fluorescence was monitored over time (a representative example for compound **1a** is reported in Supplementary Information, Fig. SI1). The fluorescence value after cells lysis was set at 100%. A fluorescence decrease was observed upon the addition of indole **1a** (10–30 μM), with a concentration effect: the higher the concentration, the more consistent fluorescence decrease.

Each BP exhibited a different chelating ability assessed by the fluorescence drop upon addition of the compound at 30 μM concentration (Fig. 3). The unsubstituted compound **1a** proved to be the most active chelating compound with a fluorescence drop of 73 ± 2.4%, followed by fluorinated compound **1b** (34 ± 2.6% cut). Other BPs (**1c**, **1e**, and CLD) reduced the fluorescence of Ca^{2+}/FURA complex of about 10% whilst ALN, **1d**, and **1f** were the less effective chelating species causing fluorescence decrease of only 5% (Fig. 3).

Thus, slight modifications to the indole moiety substituents seem to affect the chelating properties substantially. Indeed, although being considered bioisosteric, the replacement of one hydrogen with a fluorine in position 5 or 6, afforded two less effective compounds (**1b** and **1e**). Similarly, the substituent trifluoromethyl (products **1c**–**d)** caused a further loss in activity. Moreover, substitution of the indole scaffold with a pyrrolepyridine ring to give compound **1f** did not dramatically change the bisphosphonate activity with respect to ALN.

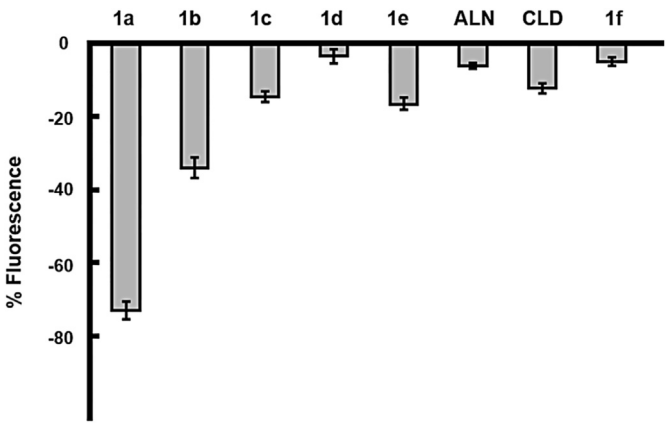

Fig. 3. Ca^{2+}/FURA complex fluorescence drop due to the addition of **1a**–**1f**, ALN, and CLD (30 μM). Data are the average of 10 experiments ± SEM.

2.2.2. BPs chelating ability of cytosolic calcium ($[Ca^{2+}]_c$) in PE/CA-PJ15 cells in Ca^{2+}-free medium

The cytosolic Ca^{2+} ($[Ca^{2+}]_c$) in the PE/CA-PJ15 cells was determined with the FURA-2 AM method [49]. The chelating ability of $[Ca^{2+}]_c$ was assessed with 10 and 30 μM BPs, in Ca^{2+} free HBSS buffer. The BPs' chelating effectiveness was evident after the first addition of BPs in the incubation medium and was confirmed by a second addition made 150 s later (e.g. Fig. SI2).

The BPs ability to chelate cytosolic calcium ion was expressed as $\Delta[Ca^{2+}]_c$ (nM) measured after 50 s from the addition (Fig. 4). The Δ

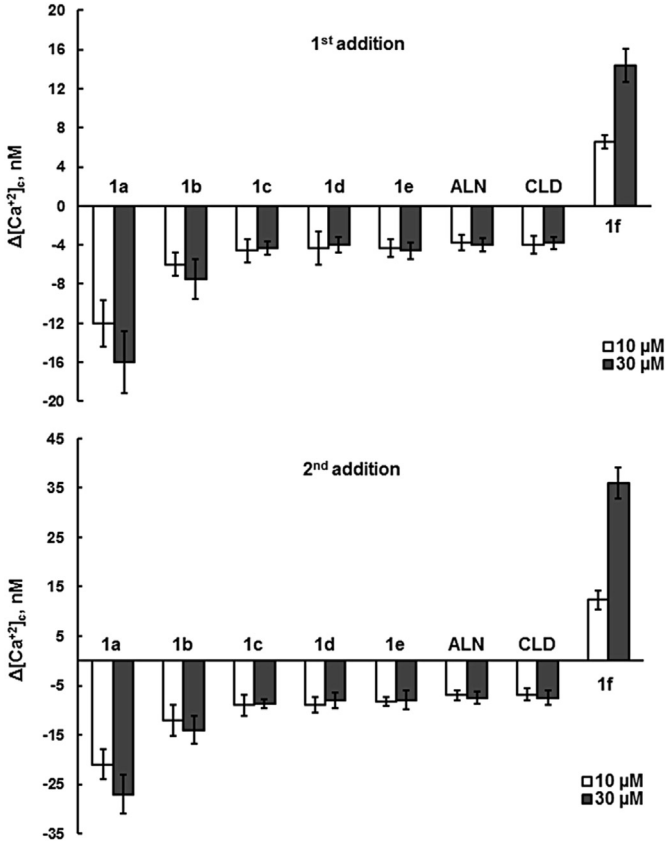

Fig. 4. BPs chelating ability of $[Ca^{2+}]_c$ in the PE/CA-PJ15 cells in Ca^{2+} free medium is expressed as decrease or increase of $[Ca^{2+}]_c$ ($\Delta[Ca^{2+}]_c$, nM). Data are expressed as the average of 10 experiments ± SEM.

$[Ca^{2+}]_c$ induced by **1a** was greater than that induced by **1b**, and by far superior to those induced by **1c**–**1e** and commercial ALN and CLD. On the contrary, azaindole **1f** did not exhibit any chelating activity, but induced a significant enhancement of the $[Ca^{2+}]_c$ levels. Thus, azacompound **1f** has a unique agonistic behavior, with respect to other IBPs, and it seems to favor the release of the ion from internal stores. Further studies are currently ongoing to examine in depth this surprising result, which to our knowledge has never been reported before.

Changes of the total $[Ca^{2+}]_c$ induced by consecutive additions of IBPs **1a**–**1f** and commercial BPs to reach a final concentration of 10 and then 30 μM were not linear. The non-linear fluorescence response at those concentration may be attributable to the different dissociation constants of the two competing complexes Fura-Ca^{2+} and BP-Ca^{2+}. In addition, a saturating effect of BPs at the nanomolar levels of $[Ca^{2+}]_c$ may be present. However, bisphosphonates, at concentrations less than 10 μM, lead to changes in $[Ca^{2+}]_c$ not measurable by this method.

2.2.3. BPs chelating ability in the PE/CA-PJ15 cells in Ca^{2+}-containing medium

In order to assess whether the presence of extracellular Ca^{2+} (as in physiological condition) affects the activity of intracellular BPs, all IBPs were further tested in presence of 1.0 mM Ca^{2+} in the incubation medium. Results are summarized in Fig. 5 where $\Delta[Ca^{2+}]_c$ values (nM) reported for all tested compounds were measured after 50 s from the addition.

Once again, indole **1a** was the most active compound in seizing $[Ca^{2+}]_c$, the effectiveness following the order: **1a** > **1b** > ALN > **1c** > CLD > **1d** > **1e** in the 10 and 30 μM BPs concentration range (Fig. 5). The diagrams in Figs. 4 and 5 clearly suggest that BPs (especially **1a** and **1b**) were able to chelate $[Ca^{2+}]_c$, even at lower concentrations of ligand (10 μM) and in the presence of Ca^{2+} in the medium (see Table 3 for a summary).

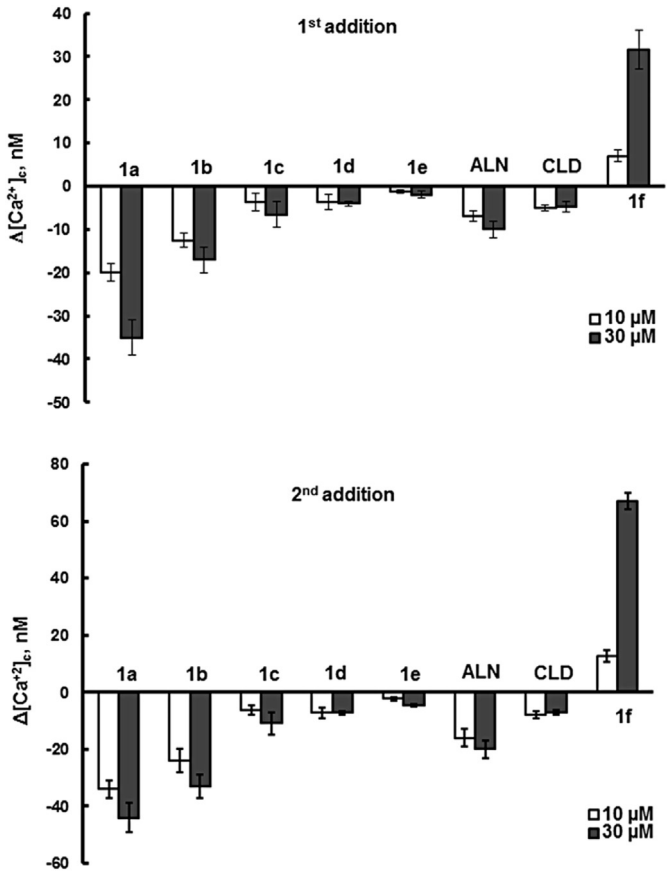

Fig. 5. $\Delta[Ca^{2+}]_c$ (nM) induced by different BPs in the PE/CA-PJ15 cells in the presence of 1 mM $[Ca^{2+}]$ in the medium. Data are the average of 10 experiments ± SEM.

Even in these experimental conditions, the aza-analog **1f** shows a peculiar behavior. Indeed, it did not show any chelating activity, and on the contrary it raised the $[Ca^{2+}]_c$ levels in a dose dependent way. The effect was even more evident than that observed in the absence of Ca^{2+} (Figs. 4 and 5). Therefore, **1f** acted as an agonist, probably by favoring the release of the ion from internal stores, also in absence of Ca^{2+} in the incubation medium. This finding might be correlated with the different nature of the indole scaffold, whereas the presence of a basic aza-group (pK_a = 7.96, predicted by MoKa [46]) provides a protonated species under physiological condition which could mimic the second messenger cADPR, by acting on the ryanodine receptors and behave as a pro-apoptotic agent.

2.3. Preliminary ADME studies

Finally, preliminary studies on the ADME properties of the BPs were performed. In particular, we evaluated the intestinal permeability in Caco-2 cells for all the tested compounds *in silico*, using the VolSurf+ software [47]. Fig. 6 shows the projection of the BPs compounds on the VolSurf+ Caco-2 model [50] for permeability prediction, generated using 750 experimental values of permeability in Caco-2 cells. The points that represent the experimental permeability values in the VolSurf+ model are colored in a blue-to-red scale, where blue and red correspond to high and low permeability, respectively. The projected BPs compounds are reported as yellow points.

The BPs compounds show a good predicted cell permeability, compared to the commercial reference compounds. In addition, substituents in the indole nucleus seem to have only a slight effect on permeability. Among the synthesized compounds, only azaindole 1f seems to demonstrate a slightly lower permeability. This effect is probably due to the presence of a basic center in the 1*H*-pyrrolo[3,2-c]pyridine ring (pK_a = 7.96 according to MoKa [46]), which is positively charged at physiological pH. This *in silico* prediction not only makes BPs promising compounds for further studies, but also suggests that the significant chelating ability detected in the cytosol might be related to a better permeability of the BPs, although the cell lines used for *in silico* and experimental studies are different.

Compounds **1a** and **1b** resulted to be the most promising compounds for their chelating ability, thus their metabolic stability was determined upon incubation in human liver microsomes for 30 min (a description of the assay is reported in the Experimental Section). Compounds **1a** and **1b** were rapidly metabolized, with the parent compounds being reduced to about 20% at the end of the incubation (See Figs. SI3 and SI4 in Supporting Information). Metabolites were identified by LC/MS analysis and a similar metabolic pathway was observed for both compounds. Indeed, compounds **1a** and **1b** underwent mono-aliphatic hydroxylation as proved by the presence of fragment 156.0808 for metabolite of compound **1a** (**1a**+**16**) and the presence of fragment 174.0714 for metabolite of compound **1b** (**1b**+**16**), (Fig. 7). Traces of the di-hydroxylated (**1a**+**32**) form were also detected for compound **1a**, suggesting that the attack occurs always at the aliphatic portion of the compound for the presence of fragment 130.0561 (Fig. 7).

3. Conclusions

Ca^{2+} is an important second messenger participating in many cellular activity. Several studies have shown that signaling

Table 3
Summary table of BPs effects on cellular Ca^{2+} in different conditions.

Comp.	% Fluorescence in Extracellular Ca^{2+}-assay[a]	$\Delta[Ca^{2+}]_c$ (Ca^{2+}-free medium), nM[b]	$\Delta[Ca^{2+}]_c$ (1 mM Ca^{2+} in the medium), nM[b]
1a	−73.0 ± 2.4	−27.0 ± 2.8	−44.0 ± 5.0
1b	−34.0 ± 2.6	−14.0 ± 2.8	−33.0 ± 4.0
1c	−16.5 ± 1.5	−8.6 ± 0.9	−11.0 ± 1.4
1d	−5.0 ± 0.5	−8.0 ± 1.0	−7.3 ± 0.5
1e	−18.0 ± 1.2	−8.0 ± 1.9	−4.6 ± 0.5
1f	−6.0 ± 1.0	+36.0 ± 3.2	+67.0 ± 3.0
ALN	−7.0 ± 0.6	−7.5 ± 1.2	−20.0 ± 3.2
CLD	−12.0 ± 1.2	−7.6 ± 1.4	−7.0 ± 0.9

[a] Values obtained after the addition of 30 mM BPs.
[b] Values obtained after the total addition of 60 mM BPs. Data are the average of 10 experiments ± SEM.

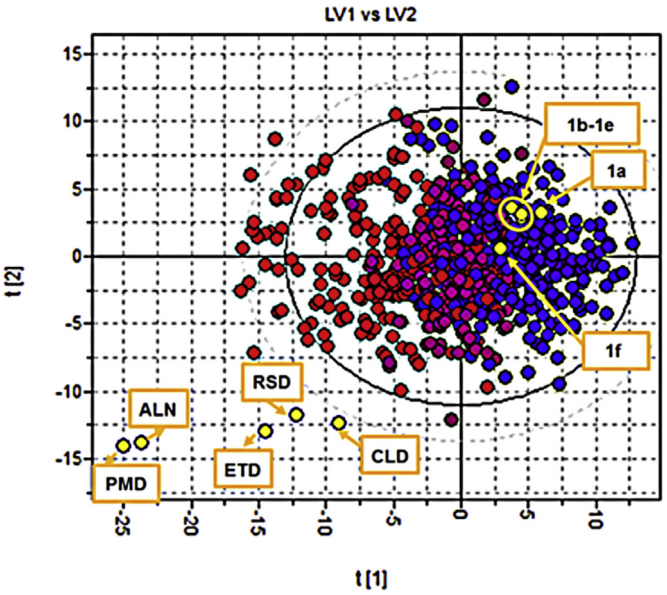

Fig. 6. Projection of the BPs in the PLS model for permeability prediction available in the VolSurf+ model (t1/t2 plot).

molecules such as Ca^{2+} are deregulated in cancer; moreover pro-apoptotic agents (as thapsigargin, staurosporine, Ca^{2+} ionophores, stress oxidative) induce cell death by interfering with Ca^{2+} homeostasis [51,52]. When physiochemical events deregulate Ca^{2+} homeostasis, Ca^{2+} acts an intrinsic stressor that may trigger cell damage [53]. The rationale of this study was to investigate the effects of commercial and synthetic bisphosphonates on extracellular and cytosolic calcium levels in human oral squamous cancer cells (PE/CA PJ-15) used as a model. Both commercial (ALN, CLD) and synthetic bisphosphonates **1a**–**f** tested in this work are able to bind extracellular Ca^{2+} but to a different extent.

The presence of the unsubstituted indole nucleus tied down to a *gem*-diphosphonate carbon (**1a**), significantly enhances the Ca^{2+} effect compared to the other tested compounds (ALN, CLD, and IBPs **1b**–**1e**). Chelating ability was also confirmed in the presence of extracellular Ca^{2+} (as in physiological conditions), where BPs showed greater activity, although not in a dose dependent manner.

Moreover the presence of fluorine in different positions on the indole showed a detrimental effect on the chelating property. Preliminary ADME studies of IBPs suggested that the cell membrane permeability has a pivotal role in cytosolic calcium binding ability with respect to commercial compounds. In addition, the presence of the indole scaffold makes these IBPs substrates for P450 cytochromes. The synthesis of a new class of chelating agents having the indole scaffold linked to the alkylbisphosphonate moiety may find a use in therapeutic doses lower than those of commercial BPs, in all those pathologies caused by a Ca^{2+} deregulated homeostasis. The long term objective of the research will be to assess the role of a new class of bisphosphonates able to modulate $[Ca^{2+}]_c$ altered during oxidative stress.

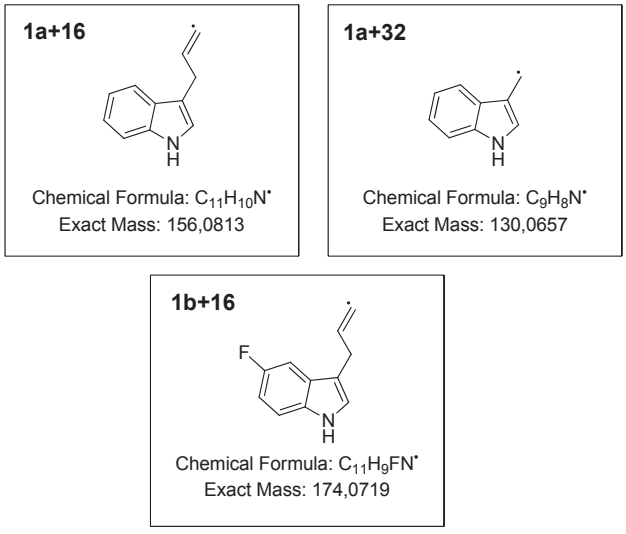

Fig. 7. Main fragments for the hydroxylated metabolites.

4. Experimental section

4.1. Chemistry

^1H NMR, ^{13}C NMR {^1H} (acquired using J-modulated (*J-MOD*) spin–echo experiments), ^{19}F NMR {^1H}, and ^{31}P NMR {^1H} were recorded on Bruker Advance II 400 MHz spectrometer at room temperature with tetramethylsilane, 85% H_3PO_4 and trichlorofluoromethane as internal standard. Chemical shifts (δ) are reported in parts per million (ppm), and peak multiplicity are reported as s (singlet), d (doublet), t (triplet), q (quartet), p (pentet), hept (heptet), m (multiplet), or br s (broad singlet). HRMS spectra were registered on Agilent Technologies 6540 UHD Accurate Mass Q-TOF LC/MS, HPLC 1290 Infinity as an external standard. IR spectra were registered in $CHCl_3$ solution in the 4000–625 cm^{-1} range. Tetraethyl ethane-1,1-bis(phosphonate) (TEBP) was prepared according to Degenhardt's protocol [41] consisting in the condensation of tetraethyl methanebis(phosphonate) with formaldehyde in the presence of diethylamine in refluxing methanol. TsOH-catalyzed elimination of methanol in refluxing toluene gave the expected product in 82% of yield.

The general procedures to prepare *N*-Boc-3-methyleneindolines **6a**–**e** was previously reported [34]. All the new precursors of the

indole bisphosphonates **1a**–**f**, were prepared as previously reported [34] and characterized as follows:

*4.1.1. tert-Butyl pyridin-4-ylcarbamate **(2f)** (74%)*

tert-butyl pyridin-4-ylcarbamate **(2f)** (74%) was prepared from 4-aminopyridine (4.00 g, 21.2 mmol) [34]. White solid. ^{1}H NMR (200 MHz, $CDCl_3$) δ 8.45 (m, 2H), 7.30 (m, 2H), 1.52 (s, 9H).

*4.1.2. tert-Butyl (3-bromopyridin-4-yl)carbamate **(3f)** (52%)*

tert-Butyl (3-bromopyridin-4-yl)carbamate (**3f**) (52%) was prepared from pyridine **2f** (2.70 g, 13.9 mmol) [34]. White solid; mp 91–92 °C. ^{1}H NMR (400 MHz, $CDCl_3$) δ 8.58 (s, 1H), 8.37 (d, J = 5.6 Hz, 1H), 8.15 (d, J = 5.6 Hz, 1H), 7.18 (s, 1H), 1.55 (s, 9H); ^{13}C NMR (101 MHz, $CDCl_3$) δ 151.6, 151.4, 149.4, 143.1, 113.1, 109.6, 82.4, 28.1 (3C).

*4.1.3. tert-Butyl (3-bromopyridin-4-yl)(prop-2-yn-1-yl)carbamate **(4f)** (69%)*

tert-Butyl (3-bromopyridin-4-yl)(prop-2-yn-1-yl)carbamate (**4f**) (69%) was prepared by alkylation of carbamate **3f** (1.90 g, 6.95 mmol) with propargyl bromide [34]. It was obtained as a brown oil after chromatography on SiO_2 (eluent, 1:1 petroleum ether/diethyl ether). ^{1}H NMR (400 MHz, $CDCl_3$) δ 8.80 (s, 1H), 8.55 (d, J = 5.1 Hz, 1H), 7.36 (bs, 1H), 4.71 (bs, 1H), 4.08 (bs, 1H), 2.25 (s, 1H), 1.43 (s, 9H); ^{13}C NMR (101 MHz, $CDCl_3$) δ 153.2, 152.6, 149.5, 147.8, 125.2, 121.7, 82.3, 78.5, 73.1, 37.8, 28.2 (3C).

*4.1.4. 1-(tert-Butoxycarbonyl)-3-methylene(pyrrolo[3,2-c]pyridine) **(5f)** (10%)*

1-(*tert*-Butoxycarbonyl)-3-methylene(pyrrolo[3,2-c]pyridine) (**5f**) (10%) was prepared by radical cyclization of propargyl pyridine **4f** (1.45 g, 4.7 mmol) [34]. After chromatography of the crude on silica gel (eluent 8:2 petroleum ether/diethyl ether) a white solid (10% yield) was collected exhibiting the following characteristics: mp 90 °C (dec). ^{1}H NMR (400 MHz, $CDCl_3$) δ 8.61 (s, 1H), 8.36 (d, J = 5.2 Hz, 1H), 7.75 (bs, 1H), 5.59 (t, J = 2.9 Hz, 1H), 5.15 (s, 1H), 4.59 (s, 2H), 1.58 (s, 9H); ^{13}C NMR (101 MHz, $CDCl_3$) δ 151.1, 150.7, 142.3, 138.5, 125.2, 109.9, 103.5, 82.0, 53.5 (2C), 28.2 (3C).

*4.1.5. General procedure for the synthesis of tetraethyl [3-(1-tert-butoxycarbonylindol-3-yl)propane-1,1-diyl]bis(phosphonates) **(6a–f)***

A mixture of the suitable *N-tert*-butoxy carbonyl-3-methyleneindoline **5a**–**f** (1.0 mmol) and VBP (1.1 mmol) was heated at 100 °C for 2–4 h in a sealed tube without solvent. The crude reaction product was washed with water (5 mL) under vigorous stirring in order to eliminate the unreacted VBP. Chromatography of the viscous residue on neutral aluminum oxide (eluent, 99:1 petroleum ether/ethanol) allowed to collect the pure product that was characterized as follows.

*4.1.5.1. 1-(tert-Butoxycarbonyl)-3-[3,3-bis(diethoxyphosphoryl)propyl]indole **(6a)** (78%).* Viscous oil; ^{1}H NMR (400 MHz, $CDCl_3$) δ 8.12 (bd, J = 7.2 Hz, 1H), 7.58 (d, J = 7.3 Hz, 1H), 7.41 (s, 1H), 7.30 (td, J = 7.2 and 1.1 Hz, 1H), 7.23 (td, J = 7.2 and 1.1 Hz, 1H), 4.45–2.25 (m, 8H), 3.00 (t, J = 7.4 Hz, 2H), 2.46–2.27 (m, 3H), 1.67 (s, 9H), 1.33 (t, J = 7.0 Hz, 6H), 1.30 (t, J = 7.0 Hz, 6H); ^{13}C NMR (101 MHz, $CDCl_3$) δ 149.7, 135.6, 130.4, 124.3, 123.0, 122.3, 119.5, 119.0, 115.2, 83.4, 62.6 (d, J = 6.7 Hz, 2C), 62.4 (d, J = 6.7 Hz, 2C), 35.9 (t, J = 133 Hz), 28.2 (3C), 25.3 (t, J = 4.8 Hz), 24.1 (d, J = 6.8 Hz), 16.3 (d, J = 5.4 Hz, 4C); ^{31}P NMR (126 MHz, $CDCl_3$) δ 25.0 (s); IR υ_{max} 2988, 2933, 1726, 1605, 1253, 1026 cm^{-1}. Elem. Anal. Calcd for $C_{24}H_{39}NO_8P_2$: C, 54.23; H, 7.40; N, 2.64. Found C, 54.27; H, 7.45; N, 2.67.

*4.1.5.2. 1-(tert-Butoxycarbonyl)-3-[3,3-bis(diethoxyphosphoryl)propyl]-5-fluoroindole **(6b)** (66%).* Viscous oil; ^{1}H NMR (400 MHz, $CDCl_3$) δ 8.06 (s, 1H), 7.44 (s, 1H), 7.22 (dd, J = 8.9 and 2.4 Hz, 1H), 7.01 (td, J = 9.1 and 2.5 Hz, 1H), 4.40–2.19 (m, 8H), 2.95 (t, J = 7.5 Hz, 2H), 2.45–2.20 (m, 3H), 1.65 (s, 9H), 1.33 (t, J = 7.0 Hz, 6H), 1.30 (t, J = 7.0 Hz, 6H); ^{13}C NMR (101 MHz, $CDCl_3$) δ 159.1 (d, J = 238 Hz), 149.4, 131.6, 131.3 (d, J = 9.3 Hz), 126.1, 119.3 (d, J = 3.9 Hz), 116.1 (d, J = 9.0 Hz), 112.0 (d, J = 25 Hz), 104.7 (d, J = 24 Hz), 83.6, 62.6 (d, J = 6.6 Hz, 2C), 62.4 (d, J = 6.7 Hz, 2C), 35.9 (t, J = 133 Hz), 28.1 (3C), 25.2 (t, J = 4.8 Hz), 24.0 (t, J = 6.7 Hz), 16.3 (d, J = 4.9 Hz, 4C); ^{19}F NMR (376 MHz, $CDCl_3$) δ −121.4 (s); ^{31}P NMR (126 MHz, $CDCl_3$) δ 24.8 (s); IR υ_{max} 2988, 1728, 1599, 1251, 1158, 1027 cm^{-1}. Elem. Anal. Calcd for $C_{24}H_{38}FNO_8P_2$: C, 52.46; H, 6.97; N, 2.55. Found C, 52.41; H, 7.10; N, 2.47.

*4.1.5.3. 1-(tert-Butoxycarbonyl)-3-[3,3-bis(diethoxyphosphoryl)propyl]-5-trifluormethylindole **(6c)** (75%).* Viscous oil; ^{1}H NMR (400 MHz, $CDCl_3$) δ 8.16 (broad d, J = 7.6 Hz, 1H), 7.78 (s, 1H), 7.48 (d, J = 8.7 Hz, 1H), 7.44 (s, 1H), 4.25–4.00 (m, 8H), 2.96 (t, J = 7.2 Hz, 2H), 2.34–2.20 (m, 3H), 1.61 (s, 9H), 1.27 (t, J = 7.1 Hz, 6H), 1.23 (t, J = 7.1 Hz, 6H); ^{13}C NMR (101 MHz, $CDCl_3$) δ 149.3, 137.2, 130.1, 124.8 (q, J = 270 Hz), 124.7, 124.7 (q, J = 32 Hz), 121.1 (q, J = 3.1 Hz), 119.7, 116.4 (q, J = 3.1 Hz), 115.5, 84.2, 62.7 (d, J = 6.7 Hz, 2C), 62.5 (d, J = 6.6 Hz, 2C), 35.9 (t, J = 133 Hz), 28.1 (3C), 25.4, 23.8 (t, J = 6.6 Hz), 16.3 (d, J = 5.8 Hz, 4C); ^{19}F NMR (376 MHz, $CDCl_3$) δ −61.4 (s); ^{31}P NMR (126 MHz, $CDCl_3$) δ 24.8 (s); IR υ_{max} 2988, 2932, 1732, 1622, 1255, 1159, 1027 cm^{-1}. Elem. Anal. Calcd for $C_{25}H_{38}F_3NO_8P_2$: C, 50.09; H, 6.39; N, 2.34. Found C, 50.16; H, 6.31; N, 2.28.

*4.1.5.4. 1-(tert-Butoxycarbonyl)-3-[3,3-bis(diethoxyphosphoryl)propyl]-6-trifluormethylindole **(6d)** (64%).* Viscous oil; ^{1}H NMR (400 MHz, $CDCl_3$) δ 7.75 (d, J = 7.7 Hz, 1H), 7.62 (d, J = 7.6 Hz, 1H), 7.39 (s, 1H), 7.33 (t, J = 7.7 Hz, 1H), 4.22 (m, 8H), 2.99 (t, J = 7.5 Hz, 2H), 2.32–2.21 (m, 3H), 1.63 (s, 9H), 1.34 (t, J = 7.1 Hz, 6H), 1.31 (t, J = 7.1 Hz, 6H); ^{13}C NMR (101 MHz, $CDCl_3$) δ 149.9, 132.9, 131.0, 126.7 (q, J = 270 Hz), 126.6, 123.5 (d, J = 5.0 Hz), 122.7, 122.1, 118.9, 112.8, 84.5, 63.1 (d, J = 6.6 Hz, 2C), 62.7 (d, J = 6.6 Hz, 2C), 35.9 (t, J = 132 Hz), 27.8 (3C), 25.3 (t, J = 6.7 Hz), 23.8 (t, J = 6.6 Hz), 16.3 (d, J = 6.2 Hz, 4C); ^{19}F NMR (376 MHz, $CDCl_3$) δ −61.0 (s); ^{31}P NMR (126 MHz, $CDCl_3$) δ 25.0 (s); IR υ_{max} 2989, 2937, 1756, 1603, 1248, 1155, 1026 cm^{-1}. Elem. Anal. Calcd for $C_{25}H_{38}F_3NO_8P_2$: C, 50.09; H, 6.39; N, 2.34. Found C, 50.18; H, 6.48; N, 2.21.

*4.1.5.5. 1-(tert-Butoxycarbonyl)-3-[3,3-bis(diethoxyphosphoryl)propyl]-6-fluoroindole **(6e)** (75%).* Viscous oil; ^{1}H NMR (400 MHz, $CDCl_3$) δ 7.77 (broad s, 1H), 7.42 (dd, J = 8.6 and 5.4 Hz, 1H), 7.32 (s, 1H), 6.91 (td, J = 8.7 and 2.4 Hz, 1H), 4.1 (m, 8H), 2.91 (t, J = 7.0 Hz, 2H), 2.43–2.24 (m, 3H), 1.60 (s, 9H), 1.26 (t, J = 7.1 Hz, 6H), 1.23 (t, J = 7.1 Hz, 6H); ^{13}C NMR (101 MHz, $CDCl_3$) δ 161.0 (d, J = 238 Hz), 158.3, 149.4, 126.7, 123.1, 119.6 (d, J = 9.7 Hz), 119.4, 110.5 (d, J = 24 Hz), 102.6 (d, J = 28 Hz), 83.8, 62.6 (d, J = 6.7 Hz, 2C), 62.4 (d, J = 6.6 Hz, 2C), 35.9 (t, J = 133 Hz), 28.1 (3C), 25.3 (t, J = 6.9 Hz), 24.0 (t, J = 6.8 Hz), 16.4 (d, J = 6.1 Hz, 2C), 16.3 (d, J = 6.2 Hz, 2C); ^{19}F NMR (376 MHz, $CDCl_3$) δ −118.1 (s); ^{31}P NMR (126 MHz, $CDCl_3$) δ 24.9 (s); IR υ_{max} 2993, 2932, 1727, 1382, 1250, 1159, 1027 cm^{-1}; Elem. Anal. Calcd for $C_{24}H_{38}FNO_8P_2$: C, 52.46; H, 6.97; N, 2.55. Found C, 52.49; H, 7.15; N, 2.42.

*4.1.5.6. 1-(tert-Butoxycarbonyl)-3-[3,3-bis(diethoxyphosphoryl)propyl]-pyrrolo[3,2-c]pyridine **(6f)** (52%).* Viscous oil. ^{1}H NMR (400 MHz, $CDCl_3$) δ 8.87 (s, 1H), 8.45 (d, J = 5.7 Hz, 1H), 7.95 (broad s, 1H), 7.42 (s, 1H), 4.2 (m, 8H), 3.05 (t, J = 7.5 Hz, 1H), 2.3 (m, 3H), 1.67 (s, 9H), 1.33 (t, J = 7.1 Hz, 6H), 1.28 (t, J = 7.1, 6H); ^{13}C NMR (101 MHz, $CDCl_3$) δ 149.1, 144.2, 142.1, 139.9, 126.6, 123.7, 118.8, 110.0, 84.6, 62.8 (2C), 62.7 (2C), 35.9 (t, J = 133 Hz), 28.1 (3C), 25.5 (t,

$J = 6.8$ Hz), 23.9 (t, $J = 6.8$ Hz), 16.4 (2C), 16.3 (2C); ^{31}P NMR (126 MHz, $CDCl_3$) δ 24.71 (s). Elem. Anal. Calcd for $C_{23}H_{38}N_2O_8P_2$: C, 51.88; H, 7.19; N, 5.26. Found C, 51.91; H, 7.29; N, 5.30.

*4.1.5.7. General procedure for the synthesis of 3-[3,3-bis(diethoxyphosphoryl)propyl]indole **1a–f**.* The suitable carbamate **6a–f** (50 mg) was cautiously heated at 150–190 °C in a sealed tube with an air heater until gas evolvement ceased (~5–10 min). After cooling, a viscous brown oil was obtained whose ^{1}H NMR spectrum was compatible with the structure of the indole bisphosphonates **1a–f**. High purity products were obtained in practically quantitative yield by flash chromatography of the crude on SiO_2 (dichloromethane/ethanol 99:1 as eluent). They were characterized as follows.

*4.1.5.8. Tetraethyl (3-(indol-3-yl)propane-1,1-diyl)bis(phosphonate) **(1a)**.* Colorless oil. ^{1}H NMR (400 MHz, $CDCl_3$) δ 8.50 (s, 1H), 7.64 (d, $J = 7.7$ Hz, 1H), 7.37 (d, $J = 8.0$ Hz, 1H), 7.22–7.08 (m, 2H), 7.06 (s, 1H), 4.26–4.02 (m, 8H), 3.08 (t, $J = 6.8$ Hz, 2H), 2.55–2.26 (m, 3H), 1.41–1.21 (m, 12H); ^{13}C NMR (101 MHz, $CDCl_3$) δ 136.5, 127.4, 122.1, 121.9, 119.1, 118.7, 114.6, 111.2, 62.5 (d, $J = 6.7$ Hz, 2C), 62.4 (d, $J = 6.7$ Hz, 2C), 35.7 (t, $J = 133$ Hz), 26.0 (t, $J = 4.8$ Hz), 24.4 (t, $J = 6.8$ Hz), 16.1 (d, $J = 3.3$ Hz, 2C), 16.3 (d, $J = 3.3$ Hz, 2C); ^{31}P NMR (126 MHz, $CDCl_3$) δ 24.1 (s, 1H); HRMS: calcd for $C_{19}H_{31}NO_6P_2$ 432.4080 ($M + H^+$), found 432.4081 ($M + H^+$).

*4.1.5.9. Tetraethyl (3-(5-fluoroindol-3-yl)propane-1,1-diyl)bis(phosphonate) **(1b)**.* Colorless oil ^{1}H NMR (400 MHz, $CDCl_3$) δ 9.30 (s, 1H), 7.20 (m, 2H), 7.02 (s, 1H), 6.83 (td, $J = 9.1$ and 2.2 Hz, 1H), 4.21–4.09 (m, 8H), 2.97 (t, $J = 7.4$, 2H), 2.3 (m, 3H), 1.28 (t, $J = 7.0$ Hz, 6H), 1.24 (t, $J = 7.0$ Hz, 6H); ^{13}C NMR (101 MHz, $CDCl_3$) 157.4 (d, $J = 234$ Hz), 133.0, 127.5 (d, $J = 9.5$ Hz), 124.0, 114.2, 111.8 (d, $J = 9.5$ Hz), 109.7 (d, $J = 26$ Hz), 103.4 (d, $J = 23$ Hz) 62.5 (d, $J = 6.7$ Hz, 2C), 62.4 (d, $J = 6.7$ Hz, 2C), 35.5 (t, $J = 133$ Hz), 25.8 (t, $J = 4.7$ Hz) 24.2 (t, $J = 6.5$ Hz), 16.2 (d, $J = 3.8$ Hz, 2C), 16.1 (d, $J = 3.8$ Hz, 2C). ^{19}F NMR (376 MHz, $CDCl_3$) δ −126.0 (s). ^{31}P NMR (126 MHz, $CDCl_3$) δ 25.17 (s); HRMS: calcd for $C_{19}H_{30}FNO_6P_2$ 450.1611 ($M+H^+$), found 450.1609 ($M+H^+$).

*4.1.5.10. Tetraethyl (3-(5-trifluoromethyl-3-yl)propane-1,1-diyl)bis(phosphonate) **(1c)**.* Colorless oil. ^{1}H NMR (400 MHz, $CDCl_3$) δ 9.76 (bs, 1H), 7.88 (s, 1H), 7.42 (d, $J = 8.6$ Hz, 1H), 7.33 (d, $J = 8.4$ Hz, 1H), 7.08 (d, $J = 2.1$ Hz, 1H), 4.19–4.05 (m, 8H), 3.06 (t, $J = 7.3$, 2H), 2.55–2.10 (m, 3H), 1.35–1.10 (m, 12H); ^{13}C NMR (101 MHz, $CDCl_3$) 138.05, 126.67, 125.56 (q, $J = 271$ Hz), 124.16, 121.20 (q, $J = 32$ Hz), 118.28 (q, $J = 3.1$ Hz), 116.34 (q, $J = 4.4$ Hz), 115,12, 111.67, 62.67 (t, $J = 7.4$ Hz, 4C), 35.70 (t, $J = 134$ Hz), 26.21(t, $J = 4.8$ Hz), 24.16 (t, $J = 7.0$ Hz), 16.31 (d, $J = 4.5$ Hz, 2C), 16.25 (d, $J = 4.5$ Hz, 2C); ^{19}F NMR (376 MHz, $CDCl_3$) δ −60.5 (s). ^{31}P NMR (126 MHz, $CDCl_3$) δ 25.07 (s); HRMS: calcd for $C_{20}H_{30}F_3NO_6P_2$ 500.1579 ($M+H^+$), found 500.1577 ($M+H^+$).

*4.1.5.11. Tetraethyl (3-(6-trifluoromethyl-3-yl)propane-1,1-diyl)bis(phosphonate) **(1d)**.* ^{1}H NMR (400 MHz, $CDCl_3$) δ 8.55 (s, 1H), 7.84 (d, $J = 7.8$ Hz, 1H), 7.46 (d, $J = 7.5$ Hz, 1H), 7.19 (s, 2H), 4.24–4.01 (m, 8H), 3.11 (t, $J = 7.1$ Hz, 2H), 2.51–2.45 (m, 3H), 1.29 (t, $J = 7.0$ Hz, 6H), 1.26 (t, $J = 7.0$ Hz, 6H); ^{13}C NMR (101 MHz, $CDCl_3$) δ 131.9, 129.0, 124.7 (q, $J = 272$ Hz), 123.2, 123.0, 119.5 (q, $J = 4.4$ Hz), 118.6, 115.4, 113.2 (q, $J = 32$ Hz), 62.6 (d, $J = 6.5$ Hz, 2C), 62.4 (d, $J = 6.5$ Hz, 2C), 35.7 (t, $J = 133$ Hz), 26.0 (t, $J = 4.6$ Hz), 23.9 (t, $J = 6.7$ Hz), 16.4 (d, $J = 5.6$ Hz, 2C), 16.3 (d, $J = 5.6$ Hz, 2C); ^{19}F NMR (376 MHz, $CDCl_3$) δ −60.87; ^{31}P NMR (126 MHz, $CDCl_3$) δ 25.07; HRMS: calcd for $C_{20}H_{30}F_3NO_6P_2$ 500.1579 ($M+H^+$), found 500.1582 ($M+H^+$).

*4.1.5.12. Tetraethyl (3-(6-fluoroindol-3-yl)propane-1,1-diyl)bis(phosphonate) **(1e)**.* Colorless oil ^{1}H NMR (400 MHz, $CDCl_3$) δ 9.75 (s, 1H), 7.93 (s, 1H), 7.45 (d, $J = 8.4$ Hz, 1H), 7.36 (d, $J = 8.4$ and 1.2 Hz, 1H), 7.14–7.01 (m, 1H), 4.24–4.11 (m, 8H), 3.08 (t, $J = 7.3$ Hz, 2H), 2.41–2.28 (m, 3H), 1.34–1.22 (m, 12H); ^{13}C NMR (101 MHz, $CDCl_3$) δ 137.9, 126.6, 124.1, 121.2 (d, $J = 32$ Hz), 118.2 (d, $J = 3.0$ Hz), 116.3 (d, $J = 4.3$ Hz), 115.1, 111.6, 62.7 (d, $J = 7.5$ Hz, 2C), 62.5 (d, $J = 7.9$ Hz, 2C), 35.6 (t, $J = 133$ Hz), 26.7 (t, $J = 5.2$ Hz), 24.0 (t, $J = 6.9$ Hz), 16.2 (d, $J = 4.0$ Hz, 2C), 16.1 (d, $J = 4.5$ Hz, 2C); ^{19}F NMR (376 MHz, $CDCl_3$) δ −60.5 (s); ^{31}P NMR (126 MHz, $CDCl_3$) δ 25.07 (s); HRMS: calcd for $C_{19}H_{30}FNO_6P_2$ 450.1611 ($M+H^+$), found 450.1610 ($M+H^+$).

*4.1.5.13. Tetraethyl (3-(3-(pyrrolo[3,2-c]pyridin-3-yl)propane-1,1-diyl)bis(phosphonate) **(1f)**.* Colorless oil ^{1}H NMR (400 MHz, $CDCl_3$) δ 8.94 (bs, 1H), 8.23 (d, $J = 5.2$ Hz, 1H), 7.34 (d, $J = 5.9$ Hz, 1H), 7.13 (s, 1H), 4.2 (m, 8H), 3.1 (m, 2H), 2.3 (m, 3H), 1.3 (m, 12H). ^{13}C NMR (101 MHz, $CDCl_3$) 142.2, 140.7, 140.2, 127.3, 124.8, 114.8, 105.0, 62.6 (d, $J = 7.9$ Hz, 2C), 62.5 (d, $J = 6.8$ Hz, 2C), 36.2 (t, $J = 133$ Hz), 26.3 (t, $J = 4.9$ Hz), 24.2 (t, $J = 6.9$ Hz), 16.4 (d, $J = 6.3$ Hz, 2C), 16.2 (d, $J = 6.0$ Hz, 2C); ^{31}P NMR (126 MHz, $CDCl_3$) δ 23.64 (s); HRMS: calcd for $C_{18}H_{30}FN_2O_6P_2$ 433.3961 ($M+H^+$), found 433.3961 ($M+H^+$).

4.2. Biological tests

4.2.1. Materials and methods

Materials Fura 2-AM (Fura-2-*pentakis*(acetoxymethyl)ester), Triton X-100 (t-octylphenoxypolyethoxyethanol), EGTA (ethylene glycol-*bis*(β-aminoethyl ether)-*N*,*N*,*N*′,*N*′-tetracetic acid), Clodronate (CLD), Alendronate (ALN), Trypan blue, and Iscove's modified Dulbecco Medium were purchased from Sigma–Aldrich corporation (St. Louis, Missouri, USA). Other reagents (reagent grade) were obtained from common commercial sources. Synthetic compounds **1a–f** were ≥98% pure as determined by UHPLC: column, Phenomenex AERIS Peptide 1.2 mm × 1000 mm (1.7 μm); flow rate, 0.8 mL/min; acquisition time, 20 min; DAD 190–650 nm; oven temperature, 45 °C; gradient of acetonitrile in water containing 0.1% of formic acid (0–100% in 20 min).

4.2.2. Cell preparations

PE/CA PJ-15 cells were cultivated (37 °C, 5% CO_2, 72 h) in Iscove-Dulbecco medium complemented (IMDM) with 1% L-glutamine, penicillin/streptomycin (100 U/mL each) and 10% inactivated fetal calf serum. The medium was replaced every 72 h and cells rinsed before use with phosphate buffered saline (PBS) to remove excess serum. The incubation medium was then discarded and the cells washed again with phosphate buffered saline (PBS). Trypsin (0.05% in 0.02% EDTA, Euroclone) was added to each flasks to detach cells. The action of trypsin was stopped after 3 min by the addition of fetal calf serum (10%). Cells were harvested by centrifugation at 400× g × 5 min and suspended in a volume of medium to obtain cell concentration of 1×10^6 cells/mL. Cell proliferation was monitored by counting the viable cells by Trypan blue exclusion method.

4.2.3. Test of Trypan blue exclusion

Aliquots (20 μL) of cell suspensions were diluted 1:10 with Trypan blue (2.22 mg/mL of PBS) and counted using a Burker chamber after standing at room temperature for 5 min. The blue-stained cells were considered as non-viable.

4.2.4. Ca^{2+} extracellular determination

The determination of the extracellular calcium was performed on an aliquot of the cell suspension (1 mL) incubated in 3 mL of HBSS (+1 mM $CaCl_2$). The cells were lysed with triton X-100. The variation of fluorescence of the sample (Ca^{2+}/FURA-2) was determined after the addition of (10–30 μM) BPs.

4.2.5. Cytosolic calcium determination

FURA-2 AM (2 μL of a 2 mM solution in DMSO) was added to

1 mL of cell suspension (about 10×10^6 cells) and incubated for 60 min at 37 °C, in the dark. Cells were then harvested by centrifugation at 800× g × 10 min and finally suspended in HBSS buffer (140 mM NaCl, 5.3 mM KCl, 1 mM $MgCl_2$, 5 mM glucose, 25 mM Hepes, adjusted to pH 7.4) to a final cell concentration of 1×10^6/mL.

An aliquot of this suspension (1 mL) was centrifuged at 800 g for 5 min, cells harvested and suspended in 3 mL of calcium-free HBSS (0.1 mM EGTA). Fluorescence was measured with a Perkin–Elmer LS 50 B spectrophotofluorometer equipped with a double excitation system (ex. 340 and 380 nm, em. 510 nm). Slit widths were set at 10 nm for excitation and 7.5 nm for emission. Cytosolic calcium concentrations ($[Ca^{2+}]_c$) were calculated as reported elsewhere [49]. When necessary, bisphosphonates and Ca^{2+} were added, as reported in the "Results" section.

4.3. Computational method

4.3.1. Permeability prediction

The VolSurf+ software (www.moldiscovery.com) was used to predict cell-permeability. The method has been extensively described elsewhere [47]. To describe the BPs compounds, the GRID [47] probes for water (OH2), hydrophobic (DRY) and H-bonding carbonyl (O) interactions were used to generate the 3D interaction energies and a grid space of 0.5 Å. The most abundant protonation state for each compound was used.

4.4. Statistical analysis

Results are expressed as means ±SEM.

4.5. Metabolism assay

Substrates were incubated with human liver microsomes (HLM, 0.5 mg protein/ml) (BD Biosciences) according to manufacturer's recommendations with minor modification. Briefly, substrates at 5 μM final concentration were preincubated in a shaking water bath for 5 min at 37 °C in 100 mM potassium phosphate buffer (pH 7.4) in a total volume of 250 μL. The reactions were initiated by addiction of 1 mM NADPH. After incubation for 0 and 30 min, 250 μL of cold acetonitrile (containing 0.6 mM labetalol as internal standard) were added to the mix to terminate the reaction. Proteins were precipitated by centrifugation at 12,000 *g* for 5 min at 4 °C, and aliquots of supernatants were analyzed by HPLC-MS/MS. The LC/MS analysis were run on a Agilent 6540 UHD accurate mass Q-TOF LC/MSMS system (Agilent Technologies, Palo Alto, CA) governed by Agilent MassHunter software (B.05.00 version). The system consists of a binary pump, autosampler, thermostated column compartment, DAD detector, source, and Q-TOF spectrometer. Chromatographic separation of the metabolites (Agilent 1290 UHPLC system) was performed with Aeris Peptide 1.7 J XB-C18, 100 × 2.1 mm (Phenomenex USA) at a constant temperature of 40 °C. The mobile phases consisted of A: H_2O/0.1% formic acid and B: acetonitrile/0.1% formic acid at the flow of 0.3 mL/min with the following gradient: Time 0 min, B 0%; Time 20 min, B 100%. The DAD Detector stored all the acquired spectra in the 10–640 nm range (2 nm spectrum step). The ion source was an Agilent Dual JetStream operating under positive ionization mode (4000 V), with as nitrogen the desolvating gas (320 °C, 10 L/min, 35 psig). The fragmentor was set to 110 V, the skimmer to 65 V, and the octrapole RF to 750 V. The spectrometric data were collected in All Ion mode in the 100·1000 mass range, with 3 scans/sec at Collision Energy of 0, 30, 40 V. The TOF operated at 2 GHz.

Acknowledgments

The authors would like to thank Prof. Renzo Ruzziconi for his scientific support and Molecular Discovery Ltd. for financial support. Dr. Cristiano Zuccaccia is kindly acknowledged for his contribution in the elucidation of NMR spectra.

Appendix A. Supplementary data

Supplementary data related to this article can be found at http://dx.doi.org/10.1016/j.ejmech.2015.08.019.

References

[1] R.E. Coleman, Metastatic bone disease: clinical features, pathophysiology and treatment strategies, Cancer Treat. Rev. 27 (2001) 165–176.
[2] H. Fleisch, Bisphosphonates in osteoporosis, Eur. Spine J. Off. Publ. Eur. Spine Soc. Eur. Spinal Deform. Soc. Eur. Sect. Cerv. Spine Res. Soc. 12 (Suppl. 2) (2003) S142–S146.
[3] H. Fleisch, J. Maerki, R.G. Russell, Effect of pyrophosphate on dissolution of hydroxyapatite and its possible importance in calcium homeostasis, proceedings of the society for experimental biology and medicine, Soc. Exp. Biol. Med. 122 (1966) 317–320.
[4] H.A. Fleisch, R.G. Russell, S. Bisaz, R.C. Muhlbauer, D.A. Williams, The inhibitory effect of phosphonates on the formation of calcium phosphate crystals in vitro and on aortic and kidney calcification in vivo, Eur. J. Clin. Invest. 1 (1970) 12–18.
[5] J. Meldolesi, T. Pozzan, The endoplasmic reticulum Ca^{2+} store: a view from the lumen, Trends Biochem. Sci. 23 (1998) 10–14.
[6] D.M. Bautista, R.S. Lewis, Modulation of plasma membrane calcium-ATPase activity by local calcium microdomains near CRAC channels in human T cells, J. Physiol. 556 (2004) 805–817.
[7] M.J. Berridge, M.D. Bootman, P. Lipp, Calcium–a life and death signal, Nature 395 (1998) 645–648.
[8] D.E. Clapham, Intracellular calcium - replenishing the stores, Nature 375 (1995) 634–635.
[9] M.R. Webster, M. Zhao, M.A. Rudek, C.L. Hann, C.L. Freel Meyers, Bisphosphonamidate clodronate prodrug exhibits potent anticancer activity in non-small-cell lung cancer cells, J. Med. Chem. 54 (2011) 6647–6656.
[10] M.J. Rogers, New insights into the molecular mechanisms of action of bisphosphonates, Curr. Pharm. Des. 9 (2003) 2643–2658.
[11] R.G. Russell, Bisphosphonates: mode of action and pharmacology, Pediatrics 119 (Suppl. 2) (2007) S150–S162.
[12] J.E. Dunford, M.J. Rogers, F.H. Ebetino, R.J. Phipps, F.P. Coxon, Inhibition of protein prenylation by bisphosphonates causes sustained activation of Rac, Cdc42, and Rho GTPases, J. Bone Miner. Res. Off. J. Am. Soc. Bone Miner. Res. 21 (2006) 684–694.
[13] P. Clezardin, F.H. Ebetino, P.G. Fournier, Bisphosphonates and cancer-induced bone disease: beyond their antiresorptive activity, Cancer Res. 65 (2005) 4971–4974.
[14] J.R. Green, Bisphosphonates: preclinical review, Oncologist. 9 (Suppl. 4) (2004) 3–13.
[15] M. Caraglia, M. Marra, C. Viscomi, A.M. D'Alessandro, A. Budillon, G. Meo, C. Arra, A. Barbieri, U.R. Rapp, A. Baldi, P. Tassone, S. Venuta, A. Abbruzzese, P. Tagliaferri, The farnesyltransferase inhibitor R115777 (ZARNESTRA) enhances the pro-apoptotic activity of interferon-alpha through the inhibition of multiple survival pathways, Int. J. Cancer. Journal International du Cancer 121 (2007) 2317–2330.
[16] M. Bezzi, M. Hasmim, G. Bieler, O. Dormond, C. Ruegg, Zoledronate sensitizes endothelial cells to tumor necrosis factor-induced programmed cell death: evidence for the suppression of sustained activation of focal adhesion kinase and protein kinase B/Akt, J. Biol. Chem. 278 (2003) 43603–43614.
[17] B. Ory, M.F. Heymann, A. Kamijo, F. Gouin, D. Heymann, F. Redini, Zoledronic acid suppresses lung metastases and prolongs overall survival of osteosarcoma-bearing mice, Cancer 104 (2005) 2522–2529.
[18] J. Liu, W. Liu, H. Ge, J. Gao, Q. He, L. Su, J. Xu, L.-q Gu, Z.-s Huang, D. Li, Syntheses and characterization of non-bisphosphonate quinoline derivatives as new FPPS inhibitors, Biochim. Biophys. Acta (BBA)-Gen. Subj. 1840 (2014) 1051–1062.
[19] D. Ledoux, Y. Hamma-Kourbali, M. Di Benedetto, A. Foucault-Bertaud, O. Oudar, O. Sainte-Catherine, M. Lecouvey, M. Kraemer, A new dimethyl ester bisphosphonate inhibits angiogenesis and growth of human epidermoid carcinoma xenograft in nude mice, Anti-Cancer Drugs 17 (2006) 479–485.
[20] G. De Rosa, G. Misso, G. Salzano, M. Caraglia, Bisphosphonates and cancer: what opportunities from nanotechnology? J. Drug Deliv. 2013 (2013) 637976.
[21] X.L. Xu, W.L. Gou, A.Y. Wang, Y. Wang, Q.Y. Guo, Q. Lu, S.B. Lu, J. Peng, Basic research and clinical applications of bisphosphonates in bone disease: what have we learned over the last 40 years? J. Transl. Med. 11 (2013) 303.
[22] R. Bergner, I.J. Diel, D. Henrich, M. Hoffmann, M. Uppenkamp, Differences in nephrotoxicity of intravenous bisphosphonates for the treatment of

malignancy-related bone disease, Onkologie 29 (2006) 534–540.
[23] I.J. Diel, R. Bergner, K.A. Grotz, Adverse effects of bisphosphonates: current issues, J. Support. Oncol. 5 (2007) 475–482.
[24] http://pusbchem.ncbi.nlm.nih.gov, in.
[25] J.J. Vepsalainen, Bisphosphonate prodrugs, Curr. Med. Chem. 9 (2002) 1201–1208.
[26] A. Townshend, D.T. Burns, R. Lobinski, E.J. Newman, G. Guilbault, Z. Marczenko, H. Onishi, Dictionary of Analytical Reagents, Taylor & Francis, 1993.
[27] G. Hagele, Z. Szakacs, J. Ollig, S. Hermens, C. Pfaff, NMR-controlled titrations: characterizing aminophosphonates and related structures, Heteroat. Chem. 11 (2000) 562–582.
[28] http://www.sanofi.ca, in.
[29] W.K. Hagmann, The many roles for fluorine in medicinal chemistry, J. Med. Chem. 51 (2008) 4359–4369.
[30] S. Purser, P.R. Moore, S. Swallow, V. Gouverneur, Fluorine in medicinal chemistry, Chem. Soc. Rev. 37 (2008) 320–330.
[31] P.V. Ramachandran, Welcome to 'fluorine in medicinal chemistry', Future Med. Chem. 1 (2009) 771–772.
[32] M. Franz, T. Hansen, P. Richter, L. Borsi, F.D. Bohmer, P. Hyckel, P. Schleier, D. Katenkamp, L. Zardi, H. Kosmehl, A. Berndt, Complex formation of the laminin-5 gamma2 chain and large unspliced tenascin-C in oral squamous cell carcinoma in vitro and in situ: implications for sequential modulation of extracellular matrix in the invasive tumor front, Histochem. Cell Biol. 126 (2006) 125–131.
[33] U.S. Singh, R. Shankar, A. Kumar, R. Trivedi, N. Chattopadhyay, N. Shakya, S. Palne, S. Gupta, K. Hajela, Synthesis and biological evaluation of indolyl bisphosphonates as anti-bone resorptive and anti-leishmanial agents, Bioorg. Med. Chem. 16 (2008) 8482–8491.
[34] F. Bellezza, A. Cipiciani, R. Ruzziconi, S. Spizzichino, Nucleus- and side-chain fluorinated 3-substituted indoles by a suitable combination of organometallic and radical chemistry, J. Fluor. Chem. 129 (2008) 97–107.
[35] S. Lepri, F. Buonerba, P. Maccaroni, L. Goracci, R. Ruzziconi, Are carboxylic esters really refractory to DAST? On the fluorination of alpha-hydroxyesters with DAST, J. Fluor. Chem. 171 (2015) 82–91.
[36] R. Ruzziconi, G. Ricci, A. Gioiello, H. Couthon-Gourves, J.P. Gourves, First general approach to cyclohex-3-ene-1,1-bis(phosphonates) by Diels-Alder cycloaddition of tetraethyl vinylidenebis(phosphonate) to 1,3-dienes, J. Org. Chem. 68 (2003) 736–742.
[37] H. Krawczyk, Indoles as nucleophiles in a self-catalytic michael reaction, Synthesis 2002 (2002) 1351–1354.
[38] M.V. Shevchuk, J.-M. Sotiropoulos, K. Miqueu, V.D. Romanenko, V.P. Kukhar, Tetrakis (trimethylsilyl) ethenylidene-1, 1-bisphosphonate: a mild and convenient Michael acceptor for the synthesis of 2-aminoethylidene-1, 1-bisphosphonic acids and their potassium salts, Synlett 2011 (2011) 1370–1374.
[39] H. Couthon-Gourvès, G. Simon, J.-P. Haelters, B. Corbel, Synthesis of novel diethyl indolylphosphonates and tetraethyl indolyl-1, 1-bisphosphonates by Michael addition, Synthesis 2006 (2006) 81–88.
[40] A. Chiminazzo, L. Sperni, M. Damuzzo, G. Strukul, A. Scarso, Copper-mediated 1,4-conjugate addition of boronic acids and indoles to vinylidenebisphosphonate leading to gem-bisphosphonates as potential antiresorption bone drugs, Chemcatchem 6 (2014) 2712–2718.
[41] C.R. Degenhardt, D.C. Burdsall, Synthesis of ethenylidenebis (phosphonic acid) and its tetraalkyl esters, J. Org. Chem. 51 (1986) 3488–3490.
[42] G.F. Smith, A.E. Walters, 194. Indoles. Part V. 3-alkylindole dimers, J. Chem. Soc. (Resumed) (1961) 940–943.
[43] E. Ascic, S.L. Buchwald, Highly diastereo- and enantioselective CuH-catalyzed synthesis of 2,3-disubstituted lndolines, J. Am. Chem. Soc. 137 (2015) 4666–4669.
[44] J. Bergman, E. Koch, B. Pelcman, Coupling reactions of indole-3-acetic acid derivatives. Synthesis of arcyriaflavin A, J. Chem. Soc. Perkin Trans. 1 (2000) 2609–2614.
[45] C. CharletFagnere, J. Laronze, J.Y. Laronze, L. Toupet, R. Vistelle, D. Lamiable, C. Mouchard, P. Renard, G. Adam, Studies on the dimerization of melatonin (5-methoxy-N-acetyltryptamine) and related compounds in acid medium. Oxidation of some 2-arylindolines into 2-arylindoles, B Soc. Chim. Fr. 133 (1996) 39–50.
[46] F. Milletti, L. Storchi, G. Sforna, G. Cruciani, New and original pKa prediction method using grid molecular interaction fields, J. Chem. Inf. Model. 47 (2007) 2172–2181.
[47] G. Cruciani, P. Crivori, P.-A. Carrupt, B. Testa, Molecular fields in quantitative structure–permeation relationships: the VolSurf approach, J. Mol. Struct. THEOCHEM 503 (2000) 17–30.
[48] K.K. Kulasekara, O.M. Lukandu, E. Neppelberg, O.K. Vintermyr, A.C. Johannessen, D.E. Costea, Cancer progression is associated with increased expression of basement membrane proteins in three-dimensional in vitro models of human oral cancer, Arch. Oral Biol. 54 (2009) 924–931.
[49] G. Grynkiewicz, M. Poenie, R.Y. Tsien, A new generation of Ca^{2+} indicators with greatly improved fluorescence properties, J. Biol. Chem. 260 (1985) 3440–3450.
[50] F. Broccatelli, G. Cruciani, L.Z. Benet, T.I. Oprea, BDDCS class prediction for new molecular entities, Mol. Pharm. 9 (2012) 570–580.
[51] S.R. Denmeade, J.T. Isaacs, The SERCA pump as a therapeutic target: making a “smart bomb” for prostate cancer, Cancer Biol. Ther. 4 (2005) 14–22.
[52] S. Weisthal, N. Keinan, D. Ben-Hail, T. Arif, V. Shoshan-Barmatz, Ca(2+)-mediated regulation of VDAC1 expression levels is associated with cell death induction, Biochim. Biophys. Acta 1843 (2014) 2270–2281.
[53] C. Cerella, M. Diederich, L. Ghibelli, The dual role of calcium as messenger and stressor in cell damage, death, and survival, Int. J. Cell Biol. 2010 (2010) 546163.